molecular weight fragments which was not done in our case and may account for the slightly lower molecular weight obtained.

Discussion

It is clear from the work reported here that bovine cardiac S1 undergoes reversible aggregation in solution and that this aggregation is the reason for the observed biphasic kinetics (Taylor & Weeds, 1976). The light-scattering results support the simple mechanism proposed to account for the S1 concentration dependence of the ATP binding process as well as the fact that the kinetics are biphasic. The light-scattering results with ATP also confirm the ATP-dependent interconversion of aggregated cardiac S1. However, the light-scattering results also show that any mechanism proposed must include higher aggregates. As pointed out under Results, the simple model proposed is oversimplified because the ATP binding and rapid hydrolysis must occur in at least two steps and the light-scattering results indicate that more than monomer and dimer species of cardiac S1 must be included. The contrast between the simple behavior of rabbit skeletal S1 (A1) in both the kinetic and light-scattering studies and the solution behavior of bovine cardiac S1 is quite striking. The steady-state rate constant, k_4, has been shown in this work to depend on protein concentration, and any future work on cardiac S1 which uses this constant as a measurable parameter should take into account the aggregation of cardiac S1. Until the complicated solution properties of cardiac S1 are completely resolved, further mechanistic studies will have to be interpreted with caution.

Acknowledgments

We thank Bill Kleese for excellent technical assistance and Howard White for many helpful discussions.

References

Foss, S. D. (1970) *Biometrics 26*, 815.
Gear, C. W. (1971) in *Numerical Initial Value Problems in Ordinary Differential Equations*, Chapter 2, Prentice-Hall, Englewood Cliffs, NJ.
Greenstadt, J. (1967) *Math. Comput. 21*, 360.
Herbert, T. J., & Carlson, F. D. (1971) *Biopolymers 10*, 2231.
Johnson, K. A., & Taylor, E. W. (1978) *Biochemistry 17*, 3432.
Margossian, S. S., & Stafford, W. F. (1979) *Biophys. J. 25*, 20a.
Taylor, R. S., & Weeds, A. G. (1976) *Biochem. J. 159*, 301.
Weeds, A. G., & Taylor, R. S. (1975) *Nature (London) 257*, 54.
Weeds, A. G., & Pope, B. (1977) *J. Mol. Biol. 111*, 129.
Weeds, A. G., Hall, R., & Spurway, N. C. (1975) *FEBS Lett. 49*, 320.

Phosphorus-31 Nuclear Magnetic Resonance Studies of Adenosine 5′-Triphosphate Bound to a Nitrated Derivative of G-Actin†

Manfred Brauer and Brian D. Sykes*

ABSTRACT: G-Actin was nitrated with tetranitromethane to form a relatively nonpolymerizable derivative. The ^{31}P NMR spectrum of ATP bound to the nitrated G-actin derivative does not differ significantly from that of ATP bound to unmodified G-actin, indicating that the nitration of Tyr-69 does not appreciably affect the ATP binding site. The relaxations times, T_1 and T_2, for the ^{31}P resonances of protein-bound ATP were measured as a function of magnetic field strength to separate the contributions of dipole–dipole and chemical shift anisotropy relaxation mechanisms. At high magnetic field strengths (8.4 T), chemical shift anisotropy was found to account for about 90% of the spin–spin relaxation rate ($1/T_2$) and about 80% of the spin–lattice relaxation rate ($1/T_1$) for all three phosphates. The effects of cross-relaxation between ^{31}P and ^{1}H nuclei are shown to be negligible for protein-bound phosphates in the nonextreme narrowing limit. On the basis of the contribution of chemical shift anisotropy to T_1 and T_2, rotational correlation times of 41, 40, and 44 ns were determined for the γ-, α-, and β-phosphates of bound ATP. Since the theoretical tumbling time for G-actin is about 36 ns, these correlation times indicate that each phosphate of ATP in the G-actin–ATP complex is tightly bound with no appreciable rapid internal mobility. Chemical shift anisotropy factors $(\Delta\sigma)(1 + \eta^2/3)^{1/2}$ were 240, 260, and 260 ppm for the bound γ-, α-, and β-phosphates, respectively. These anisotropies are higher than would be expected from model compounds and reflect interactions between the G-actin and its bound ATP. At lower magnetic field strengths, the line widths of the protein-bound phosphates are appreciably narrower and the ^{31}P–^{31}P spin coupling constants can be observed. ^{31}P NMR (36.4 MHz) spectra show a decrease in $^{2}J_{P_\alpha,P_\beta}$ from 19.6 Hz for free ATP to 12 ± 2 Hz for actin-bound ATP, also indicating some interaction between the ATP and protein.

Actin plays a central role in the structure and function of muscle. It is the major structural component of the thin filament of muscle (Oosawa & Kasai, 1971; Engel et al., 1977). Actin interacts with tropomyosin and troponin in the calcium-mediated control system for muscle contraction (McCubbin & Kay, 1980; Mannherz & Goody, 1970; Ebashi & Ebashi, 1965). The interaction of actin with the myosin heads of the thick filaments produces the force which drives the interdigitating thin and thick filaments past each other during muscle contraction (Huxley, 1969; Mannherz & Goody, 1970). Actin has also been found in virtually all nonmuscle eukaryotic cells (Clarke & Spudich, 1977), and

† From the Medical Research Council Group on Protein Structure and Function and the Department of Biochemistry, University of Alberta, Edmonton, Alberta, Canada T6G 2H7. *Received April 9, 1981.* This research was supported by the Muscular Dystrophy Association of Canada (Postdoctoral Fellowship to M.B.) and the Medical Research Council of Canada (Group on Protein Structure and Function). A preliminary report of this work was presented at a meeting of the American Society of Biological Chemists, St. Louis, MO, June 1981.

0006-2960/81/0420-6767$01.25/0

is believed to play important roles in cell motility, exocytosis, phagocytosis, chromosomal movement, and cell cleavage in mitosis and miosis and a structural role as part of the cytoskeleton of cells (Clarke & Spudich, 1977; Pollard & Weihing, 1974). Nonmuscle actin has been shown to interact with myosin (Clarke & Spudich, 1977), DNase I (Lazarides & Lindberg, 1974), profilin (Carlsson et al., 1977), spectrin (Cohen & Branton, 1979), and other proteins. Perhaps the most basic interaction of actin is with ATP, in that monomeric G-actin requires bound ATP or other purine nucleotides to maintain its native conformation (Laki et al., 1950; Straub & Feuer, 1950; Neidl & Engel, 1979). Even this relatively simple interaction is as yet incompletely understood.

^{31}P NMR has proven to be a valuable tool in the study of phosphorus-containing ligands which bind covalently or noncovalently to biological macromolecules (Cohn & Nageswara Rao, 1980; O'Neill & Richards, 1980; Withers et al., 1979; Hull et al., 1976). ^{31}P NMR studies of the binding of ATP to G-actin were initially done by Cozzone, Nelson, and Jardetzky (Cozzone et al., 1974; Nelson et al., 1974) and showed fast exchange between free and G-actin-bound ATP. Recent studies done under somewhat different conditions have indicated that the exchange is slow on the NMR time scale, with both free and bound ATP resonances clearly resolved (Brauer & Sykes, 1981).

The major disadvantage of ^{31}P NMR in the study of biological macromolecules is its lack of sensitivity. High concentrations of sample (≥0.4 mM) are required to obtain good spectra in a reasonable amount of time (12 h of data accumulation). One way to obtain higher concentrations of G-actin without incurring polymerization is to chemically modify the G-actin. Nitration of G-actin with TNM[1] was shown to selectively modify Tyr-69 (Elzinga, 1971), resulting in a nitrated derivative of G-actin for which polymerization is strongly inhibited. However, this derivative still maintains many of the other properties of actin (Lehrer & Elzinga, 1972; Chantler & Gratzer, 1975). Herein, we report a ^{31}P NMR study of the ATP bound to nitrated G-actin and compare these ^{31}P resonances with those of ATP bound to unmodified G-actin (Brauer & Sykes, 1981). The T_1 and T_2 values of these resonances at different magnetic field strengths are reported and analyzed in terms of the various relaxation mechanisms. In particular, chemical shift anisotropy (CSA), which plays a predominant role in ^{19}F relaxation mechanisms (Hull & Sykes, 1975a,b), is shown to have a predominant role in relation with ^{31}P NMR at high magnetic fields. Cross-relaxation, which has been shown to have significant effects on proton and ^{19}F T_1 and NOE measurements in proteins (Sykes et al., 1978; Hull & Sykes, 1975a,b), is shown to have a negligible effect on the measurement of T_1 for relatively isolated ^{31}P nuclei, such as those of protein-bound nucleotide phosphates.

Theory

There are several possible relaxation mechanisms contributing to the nuclear spin relaxation rates ($1/T_1$ and $1/T_2$) for phosphorus nuclei on proteins. These are dipole–dipole (DD) interactions of the phosphorus nucleus with other phosphorus nuclei (PP) or with proton nuclei (HP), chemical shift anisotropy (CSA) relaxation, and chemical exchange (EX). Spin–rotation interactions are only important for very short correlation times ($\tau_c < 10^{-11}$ s) and can be ignored for macromolecular systems.

We consider first the contributions of the four above-mentioned mechanisms to the spin–spin relaxation rate ($1/T_2$). The dipolar relaxation between two phosphorus nuclei is given by (Solomon, 1955; Abragam, 1961)

$$\frac{1}{T_{2,\mathrm{DD}}^{\mathrm{PP}}} = \frac{3}{20}\left(\frac{\gamma_P^4\,\hbar^2}{r_{PP}^6}\right)[3J(0) + 5J(\omega_P) + 2J(2\omega_P)] \quad (1)$$

where the spectral density $J(\omega)$ is defined by $J(\omega) = \tau_c/[1 + (\omega\tau_c)^2]$ for an isotropically tumbling molecule, τ_c is the rotational correlation time, ω_P is the Larmor frequency of the ^{31}P nucleus (in radians per second), γ_P is the gyromagnetic ratio of the ^{31}P nucleus, and r_{PP} is the distance between the ^{31}P nuclei. For large proteins and high magnetic field strengths, the rotational correlation time will be long and the nuclear spins will be in the nonextreme narrowing limit defined by $(\omega\tau_c)^2 \gg 1$. In this limit, the phosphorus–phosphorus dipolar contribution to T_2 is given by

$$\frac{1}{T_2^{\mathrm{PP}}} = \frac{9}{20}\left(\frac{\gamma_P^4\,\hbar^2}{r_{PP}^6}\right)\tau_c \quad (2)$$

The contribution of dipolar interactions between the phosphorus nucleus and proton nuclei is given, for each proton, by (Solomon, 1955; Abragam, 1961)

$$\frac{1}{T_2^{\mathrm{HP}}} = \frac{1}{20}\left(\frac{\gamma_H^2\gamma_P^2\hbar^2}{r_{HP}^6}\right) \times [4J(0) + J(\omega_H - \omega_P) + 3J(\omega_P) + 6J(\omega_H) + 6J(\omega_H + \omega_P)] \quad (3)$$

where γ_H is the gyromagnetic ratio for the ^{1}H nucleus, r_{HP} is the distance between the phosphorus and the particular proton considered, and ω_H is the Larmor frequency of the ^{1}H nucleus. In the nonextreme narrowing limit, this contribution simplifies to

$$\frac{1}{T_2^{\mathrm{HP}}} = \frac{1}{5}\left(\frac{\gamma_H^2\gamma_P^2\hbar^2}{r_{HP}^6}\right)\tau_c \quad (4)$$

The contribution of chemical shift anisotropy to the relaxation of phosphorus nuclei is given by (Gutowsky & Woessner, 1956; Abragam, 1961)

$$1/T_{2,\mathrm{CSA}} = \tfrac{2}{90}\omega_P^2(\Delta\sigma)^2(1 + \eta^2/3)[4J(0) + 3J(\omega_P)] \quad (5)$$

where $\Delta\sigma$ is the anisotropy of the chemical shift, and η is the asymmetry term [see Hull & Sykes (1975a,b)], which reduces in the nonextreme narrowing limit to

$$1/T_{2,\mathrm{CSA}} = \tfrac{4}{45}\omega_P^2(\Delta\sigma)^2(1 + \eta^2/3)\tau_c \quad (6)$$

If we neglect cross-correlation between the relaxation mechanisms (Werbelow & Marshall, 1974, 1975), the above three contributions can be added to give the T_2 relaxation rate ($1/T_{2B}$) for the protein-bound phosphorus nucleus.

We must now consider the effect of the chemical exchange of the phosphorus between its bound and unbound states, which for this specific case is represented by

$$\mathrm{ATP} + \text{G-actin} \underset{k_{-1}}{\overset{k_1}{\rightleftharpoons}} \mathrm{ATP{\cdot}G\text{-}actin} \quad (7)$$

where k_1 and k_{-1} are association and dissociation rate constants. Since separate resonances are observed for the free (F) and bound (B) ATP, the chemical exchange is in the slow exchange case, $(\tau_B\Delta)^2 > 1$, where τ_B is the lifetime of the

[1] Abbreviations used: TNM, tetranitromethane; CSA, chemical shift anisotropy relaxation; DD, dipole–dipole relaxation; Tris, tris(hydroxymethyl)aminomethane; DTT, dithiothreitol; NaDodSO$_4$, sodium dodecyl sulfate; T_1, spin–lattice relaxation time; T_2, spin–spin relaxation time.

bound ATP ($\tau_B = 1/k_{-1}$) and Δ is the chemical shift difference (in radians per second) between the bound and free ATP resonances. The observed T_2 relaxation rate of the bound resonance is given by

$$1/T_{2,OBS} = 1/T_{2B} + 1/\tau_B = 1/T_{2B} + k_{-1} \quad (8)$$

We now consider the relative contributions of the various relaxation mechanisms to the spin–lattice relaxation rate $1/T_1$. This problem is further complicated in principle by cross-relaxation, but we shall show that these effects are negligible for protein-bound phosphorus nuclei and that single exponential relaxation is expected. The first mechanism is the dipolar interaction between two phosphorus nuclei. The spin–lattice relaxation of this two-spin system is represented by two coupled differential equations (Solomon, 1955; Abragam, 1961). However, in the limit where the observed relaxation rates are approximately equal, cross-relaxation can be neglected (Campbell & Freeman, 1973), and the spin–lattice relaxation rate due to dipolar interactions between phosphorus nuclei is given by (Solomon, 1955; Abragam, 1961)

$$\frac{1}{T_{1,DD}^{PP}} = \frac{3}{10}\left(\frac{\gamma_P^4\hbar^2}{r_{PP}^6}\right)[J(\omega_P) + 4J(2\omega_P)] \quad (9)$$

which in the nonextreme narrowing limit can be written as

$$\frac{1}{T_{1,DD}} = \frac{3}{5}\left(\frac{\gamma_P^4\hbar^2}{r_{PP}^6}\right)\left(\frac{1}{\omega_P^2\tau_c}\right) \quad (10)$$

The dipolar interaction of the phosphorus nucleus by surrounding proton nuclei must also be written formally as a set of coupled differential equations. The effects of cross-relaxation between the phosphorus and proton nuclei and of spin diffusion among the proton nuclei on the relaxation behavior must be considered. Hull & Sykes (1975a,b) have worked this problem out in detail for proton–fluorine interactions, and their equations are equally valid for any other nucleus. We can describe the problem in terms of a sum of two-spin interactions between the I nucleus (^{31}P) and k different S nuclei (^{1}H's) and represent the spin–lattice relaxation of the ^{31}P nuclei as (Solomon, 1955)

$$\frac{dI_z}{dt} = -(\rho_{IS} - \rho^*)(I_z - I_0) - \sum_k \sigma_{IS}^k(S_z^k - S_0^k) \quad (11)$$

where I_z and S_z are the longitudinal components of the magnetic moments at time t, and I_0 and S_0 are the corresponding components at equilibrium, ρ_{IS} and σ_{IS} are dipolar relaxation rates, and ρ^* represents other relaxation mechanisms. Hull & Sykes have shown for a single fluorine nucleus in a protein (even without the inclusion of other relaxation mechanisms ρ^*) that cross-relaxation can be neglected and the observed fluorine relaxation is a single exponential with a rate given at $1/T_1 = \rho_{IS} + \rho^*$. This results from the fact that the proton spin reservoir always remains near equilibrium $(S_z - S_0) \simeq 0$ because of the large number of protons, the efficient spin diffusion among the protons, and the rapid independent relaxation of the proton spins. The case is even stronger for phosphorus because of the relative reduction in the cross-relaxation rate as a function of the difference in frequency between the nuclei involved. This is, in the nonextreme narrowing limit

$$\frac{\rho_{IS}}{\sigma_{IS}} = \frac{3 + [1/(1 - \gamma_H/\gamma_x)^2] + [6/(1 + \gamma_H/\gamma_x)^2]}{[6/(1 + \gamma_H/\gamma_x)^2) - [1/(1 - \gamma_H/\gamma_x)^2]} \quad (12)$$

which equals −1.02 when X = ^{19}F but 112 when X = ^{31}P. Further, there are in general no nearby protons, so dipolar interactions are reduced relative to other mechanisms such as chemical shift anisotropy; the smaller γ_P relative to γ_H means that relaxation of the proton bath will be even more efficient relative to phosphorus–proton interactions. The contribution of phosphorus–proton dipolar interactions is thus given by

$$\frac{1}{T_{1,DD}} = \frac{1}{10}\left(\frac{\gamma_P^2\gamma_H^2\hbar^2}{r_{HP}^6}\right)[J(\omega_H - \omega_P) + 3J(\omega_P) + 6J(\omega_H + \omega_P)] \quad (13)$$

which in nonextreme narrowing becomes

$$\frac{1}{T_{1,DD}^{PH}} \simeq \left(\frac{0.4\gamma_P^2\gamma_H^2\hbar^2}{r_{HP}^6}\right)\left(\frac{1}{\omega_P^2\tau_c}\right) \quad (14)$$

The contribution of chemical shift anisotropy to the spin–lattice relaxation is given by

$$1/T_{1,CSA} = \tfrac{2}{15}\omega_P^2(\Delta\sigma)^2(1 + \eta^2/3)J(\omega_P) \quad (15)$$

which in nonextreme narrowing becomes

$$1/T_{1,CSA} = \tfrac{2}{15}(\Delta\sigma)^2(1 + \eta^2/3)(1/\tau_c) \quad (16)$$

The observed T_1 of the bound ATP resonances, again neglecting cross-correlation between the various relaxation mechanisms and in the absence of chemical exchange, is thus given by the sum of eq 10, 14, and 16. If chemical exchange is slow not only on the chemical shift time scale as above but also on the T_1 time scale (τ_B/T_{1B}, $\tau_B/T_{1F} > 1$) so that different T_1's are measured for the free and bound ATP resonances, then the observed T_1 of the bound ATP resonance is given by

$$1/T_{1,OBS} = 1/T_{1B} + 1/\tau_B = 1/T_{1B} + k_{-1} \quad (17)$$

Materials and Methods

Actin was prepared from rabbit skeletal muscle by the method of Spudich & Watt (1971). The G-actin was nitrated by reacting a 20-fold excess of TNM with 5 mg/mL G-actin at pH 8.0 at room temperature for 15 min (Elzinga, 1971). The sample was then dialyzed against a buffer of 2 mM Tris, 0.2 mM $CaCl_2$, 0.5 mM DTT, and 0.2 mM ATP, pH 7.8, at 4 °C for 2–3 days. Residual F-actin was removed by ultracentrifugation at 80000g for 3 h at 4 °C, and nitrated G-actin was concentrated and prepared for ^{31}P NMR as described previously (Brauer & Sykes, 1981). Determinations of pH, indicated as pH*, were uncorrected for the deuterium isotope effect.

Nitrated G-actin migrated in one band on $NaDodSO_4$–gel electrophoresis (Weber & Osborn, 1969), indicating no detectable contaminating nonactin protein or intramolecular cross-linking during the nitration reaction (Vincent et al., 1970). To check for denatured actin aggregates, gel filtration was done by using Sephadex G-200 equilibrated in normal dialysis buffer at 4 °C (Adelstein et al., 1963; Rees & Young, 1967); over 90% of the nitrated G-actin was found to be monomeric. Amino acid analyses of the nitrated G-actin were done on a Durrum D-500 amino acid analyzer. Viscosities were measured with an Ostwald viscometer with a flow time for water of 274 s.

^{31}P NMR (109.3 MHz) spectra were taken as described previously (Brauer & Sykes, 1981). Spectra were also taken at 162.0 MHz on a Bruker WH-400/DS NMR spectrometer, at 81.0 MHz on a Bruker WH200 NMR spectrometer, and 36.4 MHz on a Bruker HFX10 NMR spectrometer (90 MHz

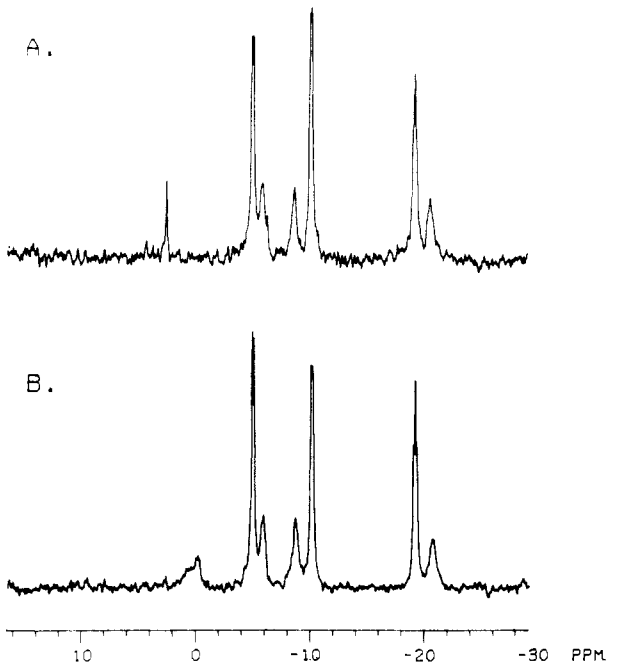

FIGURE 1: 109.3-MHz ^{31}P NMR spectra of G-actin and nitrated G-actin. Both samples were run at pH* 7.8, 4 °C, in 1 mM Tris, 0.25 mM DTT, 0.1 mM $CaCl_2$, and 50% D_2O. Both samples contained free ATP in a molar ratio of 0.5 mol of free ATP to 1.0 mol of protein. (A) G-Actin (0.40 mM) (35 300 scans) (10-Hz line broadening). (B) Nitrated G-actin (0.85 mM) (20 000 scans) (10-Hz line broadening).

for ^1H NMR). T_2 values were determined from the line widths of the protein-bound ATP resonances after correction for the line broadening caused by computer digital filtering and the multiple character of the resonance resulting from spin–spin coupling. T_1 values were determined on the basis of the progressive saturation method (Freeman & Hill, 1971). No ^1H decoupling was used in acquiring any of the ^{31}P NMR spectra unless specifically indicated.

Results

Amino acid analyses of the nitrated G-actin after 24 h of acid hydrolysis showed the presence of 1.5 ± 0.1 mol of nitrotyrosine per mol of G-actin. This compares reasonably well with the 1.2 mol of nitrotyrosine per mol of G-actin found previously (Elzinga, 1971). Viscosity studies showed that the polymerizability of the nitrated G-actin was inhibited. While 0.1 M KCl caused a 0.66 mg/mL solution of G-actin to polymerize completely within 90 min at 20 °C, no increase in viscosity was seen for a similar solution of nitrated G-actin over 24 h. $MgCl_2$ (0.2 mM) caused the rapid polymerization of 0.66 mg/mL G-actin within 10 min, but again no detectable polymerization of nitrated G-actin occurred over 24 h under the same conditions.

The ^{31}P NMR spectrum of nitrated G-actin plus free ATP was obtained (Figure 1B) and compared to that of unmodified G-actin (Figure 1A). In Figure 1A, the sharp resonances at −5.0, −10.1, and −19.3 ppm from 85% phosphoric acid were assigned to the γ-, α-, and β-phosphates, respectively, of free ATP; the broader resonances at −5.9, −8.7, and −20.6 ppm were assigned to the γ-, α-, and β-phosphates, respectively, of G-actin-bound ATP (Brauer & Sykes, 1981). The spectrum of nitrated G-actin (Figure 1B) looks very similar to that of the unmodified G-actin (Figure 1A). Thus, the sharp resonances in Figure 1B at −5.0, −10.2, and −19.3 ppm were assigned to the γ-, α-, and β-phosphates of free ATP, and the broad resonances at −5.9, −8.7, and −20.7 ppm were assigned to the γ-, α-, and β-phosphates of ATP bound to nitrated G-actin. The chemical shifts of the three ^{31}P resonances of ATP bound to G-actin and to nitrated G-actin agree within 0.1 ppm. The observed line widths of the G-actin-bound ATP resonances (corrected for the 10-Hz line broadening but not corrected for spin–spin splittings) were 52, 49, and 68 Hz for the γ-, α-, and β-phosphates, respectively; the corresponding line widths found for nitrated G-actin on the basis of several different preparations were 54, 51, and 68 Hz for the γ-, α-, and β-phosphates. Thus, the line widths of the protein-bound ATP resonances were the same (±5 Hz) for G-actin and nitrated G-actin. Since both the free and bound ATP resonances are seen in Figure 1B, the exchange of ATP between its free and protein-bound sites is slow on the NMR time scale for both nitrated G-actin and unmodified G-actin (Brauer & Sykes, 1981). Thus, the nitration of Tyr-69 does not appreciably alter the chemical shifts, line widths, or observable exchange kinetics of the ATP bound to G-actin.

Two significant differences exist between the ^{31}P NMR spectra of the G-actin and nitrated G-actin systems. Figure 1A has a sharp resonance at +2.4 ppm, which corresponds to inorganic phosphate released due to the polymerization of some of the G-actin (Brauer & Sykes, 1981). This resonance is not present in Figure 1B, indicating that no appreciable polymerization has occurred in the nitrated G-actin. There is, however, a rather broad resonance at −0.2 ppm in the spectrum of nitrated G-actin, which is absent in the spectrum of unmodified G-actin. The magnitude of this resonance varied from one preparation of nitrated G-actin to the next; in some preparations, this peak was not observed at all. This resonance may be due to some phosphorylation of the nitrated G-actin during its reaction with TNM at room temperature (Grazi & Magri, 1979). Alternatively, it may be due to the noncovalent binding of inorganic phosphate or ADP to a weak secondary binding site on the nitrated G-actin. In the possible case of ADP binding, ADP has been shown to bind to myosin subfragment-1, giving a resonance at about 0 ppm (Shriver & Sykes, 1981).

The sample of nitrated G-actin for which the 109.3-MHz ^{31}P spectrum is shown in Figure 1B was also analyzed at 162.0, 81.0, and 36.4 MHz. The resultant spectra of the free and protein-bound resonances of the γ-, α-, and β-phosphates of ATP are shown in parts A, B and C of Figure 2, respectively. The spectra are plotted on an arbitrary chemical shift scale in hertz, rather than parts per million, to show the actual line-width increase of the protein-bound resonances with increasing magnetic field strength. This increase in line width with increasing field strength reflects the contribution of CSA to the total spin–lattice relaxation rate (T_2^{-1}) (See eq 5 and 6).

The observed line widths of the protein-bound ATP resonances in Figure 2 include a contribution due to the homonuclear spin–spin splitting patterns. At low magnetic field strength, where the line widths are narrowest, it was possible to resolve these splittings. Figure 3 shows 36.4-MHz spectra of nitrated G-actin at 28 and 4 °C. One can observe a doublet with a splitting of 19 ± 2 Hz for the γ-phosphate, a doublet with a 9 ± 2 Hz splitting for the α-phosphate, and an apparent triplet with a 12 ± 2 Hz splitting for the β-phosphate. By use of spectral simulation of the α-phosphate doublet, the actual $^2J_{P_\alpha, P_\beta}$ splitting was found to be 12 ± 2 Hz, while the $^2J_{P_\beta, P_\gamma}$ became 20 ± 2 Hz for the γ-phosphate. When these coupling constants were used, the resonance for the β-phosphate could be simulated; the resulting line shape was an overlapping doublet of doublet patterns, with the two central resonances

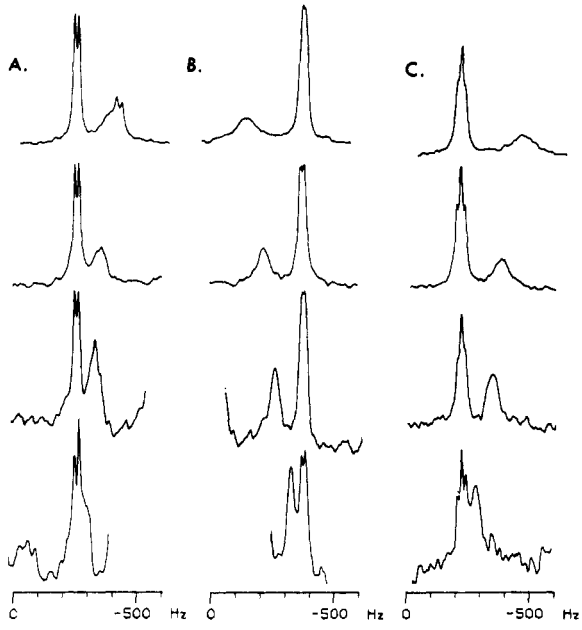

FIGURE 2: ^{31}P NMR spectra of nitrated G-actin at various magnetic field strengths. Spectra were taken at 162.0, 109.3, 81.0, and 36.4 MHz (top to bottom). All spectra were taken of the sample of nitrated G-actin described in Figure 1B at a temperature of 4 °C. Line broadening of 10 Hz was used for all spectra to decrease spectral noise. The spectral are plotted on an arbitrary chemical shift scale in hertz to facilitate the measurement of line widths. The free ATP resonances are aligned in each case. The 162.0- and 109.3-MHz spectra were obtained from 15 000 scans, the 81.0-MHz spectrum was obtained from 20 000 scans, and the 36.4-MHz spectrum was obtained from 30 000 scans. (A) γ-Phosphates of free and protein-bound ATP (left to right) (the sharp doublet resonance on the bound γ-phosphate resonance at 162.0 MHz is due to the β-phosphate resonance of a small amount of free ADP). (B) α-Phosphates of protein-bound and free ATP (left to right). (C) β-Phosphates of free and protein-bound ATP (left to right).

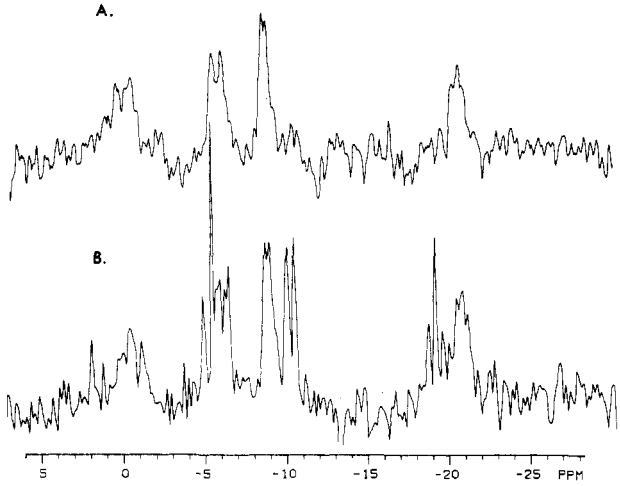

FIGURE 3: 36.4-MHz ^{31}P NMR spectra of nitrated G-actin. Samples contained 0.8 mM nitrated G-actin in 1 mM Tris, 0.25 mM DTT, and 0.1 mM $CaCl_2$ in 50% D_2O, pH* 7.8. A line broadening of 2 Hz was used to decrease spectral noise. (A) Nitrated G-actin at 28 °C (20 000 scans). Broad-band ^{1}H decoupling was used in this spectrum. (B) Nitrated G-actin at 4 °C (60 000 scans). Some free ATP was present in this sample, as indicated by the sharp resonances at −5.0, −10.2, and −19.3 ppm.

unresolved and with an apparent splitting for the two outside resonances which corresponded to the apparent splitting seen in Figure 3 for the β-phosphate resonance. By subtracting these splittings from the observed line widths of the protein-bound ATP resonances, one can determined the true line widths of these resonances.

Table I: T_2 Values for ^{31}P Resonances of ATP Bound to Nitrated G-Actin

frequency (MHz)	P_γ (ms)	P_α (ms)	P_β (ms)
36.4	20 ± 3	20 ± 2	25 ± 5
81.0	12 ± 3	9.9 ± 0.6	11 ± 2
109.3	8.2 ± 0.9	6.9 ± 1.0	6.5 ± 0.3
162.0	3.8 ± 0.2	3.4 ± 0.2	3.4 ± 0.1

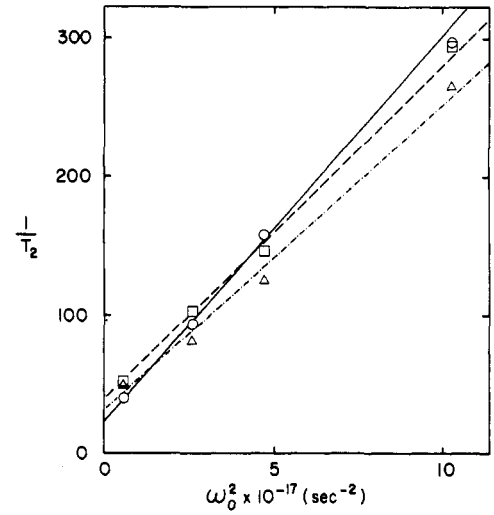

FIGURE 4: Plot of $1/T_2$ vs. ω_0^2 for ^{31}P resonances of ATP bound to nitrated G-actin. $1/T_2$ values were determined from the line widths of the protein-bound ATP resonances of nitrated G-actin at 4 °C (Figure 2), corrected for the homonuclear spin–spin splittings (Figure 3). (△) γ-Phosphate; (□) α-phosphate; (○) β-phosphate.

The line widths of the ATP resonances in Figure 3 did not increase significantly between 4 and 28 °C. This indicates that we are in the very slow exchange limit at 4 °C for the transition of ATP between its free form and its protein-bound form, so that contribution of chemical exchange ($1/\pi\tau_B$) to the bound linewidth ($1/\pi T_{2B}$) is negligible ($1/T_{2B} \gg 1/\tau_B$). As further support, we will show below that different T_1's are measured for the free and bound ATP phosphates. This implies that $\tau_B/T_{1B} > 1$. Since $T_{1B} > T_{2B}$ for all phosphates, then $\tau_B/T_{2B} \gg 1$.

From the line widths of the protein-bound ATP resonances in Figure 2, corrected for the homonuclear spin–spin splittings observed in Figure 3, values for T_2 were determined (Table I). In Figure 4, $1/T_2$ was plotted against ω_0^2. Since $T_1 \gg T_2$ for all the bound phosphate resonances (see below), the NMR relaxation is outside of the extreme narrowing limit. In this limit, the contribution of CSA to the spin–spin relaxation rate is directly proportional to ω_0^2, while the DD contributions are independent of ω_0^2, while the DD contributions are independent of ω_0^2 (see eq 2, 4, and 6); thus, the value of $1/T_2$ extrapolated to zero magnetic field strength represents $1/T_{2,DD}$. One can see from Figure 4 that at high magnetic field strengths, CSA is the dominant relaxation process for all three phosphates. For example, at 162.0 MHz, CSA accounts for 88%, 87%, and 92% of the total corrected line widths of the γ-, α-, and β-phosphate resonances, respectively, of the bound ATP.

T_1 values for the ^{31}P resonances of the free and protein-bound ATP were determined at 36.4, 109.3, and 162.0 MHz by progressive saturation, using the same sample as was used in Figure 2. The results are shown in Table II. It should be noted that at 109.3 and 162.0 MHz, the T_1 values for the bound ATP resonances are quite long (3.1–4.4 s), while the free ATP resonances have significantly shorter T_1 values

Table II: T_1 Values for ^{31}P Resonances of ATP Bound to Nitrated G-Actin and Free ATP

frequency (MHz)	P_γ (s)	P_α (s)	P_β (s)
	Protein-Bound ATP		
36.4	0.8 ± 0.1	1.0 ± 0.1	1.0 ± 0.1
109.3	3.1 ± 0.3	3.3 ± 3.9	3.9 ± 0.3
162.0	4.4 ± 0.3	3.7 ± 0.3	3.7 ± 0.2
	Free ATP		
36.4	0.9 ± 0.1	1.1 ± 0.1	1.9 ± 0.1
109.3	1.0 ± 0.2	0.7 ± 0.2	0.8 ± 0.2
162.0	0.7 ± 0.2	0.5 ± 0.2	0.5 ± 0.2

(0.5–1.0 s). This indicates that there is slow exchange between the free and protein-bound ATPs with respect to T_1 values as well as slow exchange with respect to T_2 values. In Figure 5, $1/T_1$ is plotted against $1/\omega_0^2$. In this plot, the slope represents the contribution of $1/T_{1,DD}$, while the CSA contribution is independent of magnetic field strength (see eq 10, 14, and 16). The value of $1/T_1$ extrapolated to $1/\omega_0^2$ equal to zero (infinite magnetic field strength) gives the contribution of CSA to the spin–lattice relaxation rate. Figure 5 indicates that at high magnetic field strengths, CSA is the dominant relaxation process governing T_1 values as well as T_2 values. For example, at 162.0 MHz, CSA accounts for 78%, 85%, and 82% of the total rate of spin–lattice relaxation of the γ-, α-, and β-phosphate resonances, respectively.

The observed spin–spin and spin–lattice relaxation rates are sums of the contributions of CSA and DD to these rates. Thus, from the observed T_2 (Table I) and T_1 (Table II) values, and from the values of $1/T_{2,DD}$ (Figure 4) and $1/T_{1,CSA}$ (Figure 5), which are both independent of magnetic field strength, one can readily calculate the $1/T_{2,CSA}$ and $1/T_{1,DD}$ values (Table III).

Since CSA is the dominant relaxation mechanism of both T_1 and T_2 processes at high magnetic field strengths, we will combine the equations describing the dependence of T_1 and T_2 on CSA to obtain an estimate of τ_c for the phosphates of protein-bound ATP and the chemical shift anisotropy term $(\Delta\sigma)(1 + \eta^2/3)^{1/2}$. Combining eq 6 and 16, the contributions of CSA to $1/T_2$ and $1/T_1$ in the nonextreme narrowing limit, we can solve for τ_c and $(\Delta\sigma)(1 + \eta^2/3)^{1/2}$. When the values of $1/T_{1,CSA}$ and $1/T_{2,CSA}$ are used at various magnetic field strengths in Table III, values for τ_c and $(\Delta\sigma)(1 + \eta^2/3)^{1/2}$ were calculated (Table III).

Discussion

The calculated τ_c values for γ-, α-, and β-phosphates of protein-bound ATP in Table III are comparable to those expected for a protein the size of G-actin. When the τ_c values determined at 109.3 and 162.0 MHz are used, the average correlation times for the γ-, α-, and β-phosphates are 41, 40, and 44 ns, respectively. The values determined at 36.4 MHz are less accurate since the $1/T_{2,CSA}$ term is smaller and subject to more experimental error. Typical literature values for the experimentally determined τ_c of G-actin range from 39 to 55 ns (Mihashi & Wahl, 1975; Ikkai et al., 1979; Tao, 1978; Cheung et al., 1971), while the theoretical τ_c for G-actin based on the Strokes–Einstein equation is 36 ns (Brauer & Sykes, 1981). Thus, the τ_c values determined here for the three phosphates of ATP reflect the rotational motion of the entire protein, indicating that all three phosphates of G-actin-bound ATP are rigidly bound with no appreciable rapid internal mobility. This conclusion should not be too surprising in view of the progressively stronger binding of adenosine, AMP, ADP, and ATP to G-actin. Adenosine itself does not bind appreciably to G-actin (Oosawa & Kasai, 1971). The binding of ADP to G-actin was found to be 2500-fold stronger than the binding of AMP, and the binding of ATP was found to be more than 8-fold stronger than the binding of ADP (Cooke & Murdoch, 1973). More recently, the binding constant for ATP has been found to be 175-fold higher than that of ADP (Neidl & Engel, 1979). If one of the phosphates of ATP were not involved in the binding to G-actin, then one would not expect to see a 2–3 order of magnitude increase in binding with the addition of each phosphate to the adenine nucleotide. ATP analogues in which a nitrogen or carbon was substituted for an oxygen (e.g., AMPPNP, AMPPCP, and CMPCPP) exhibited weaker binding than ADP, indicating the selectivity

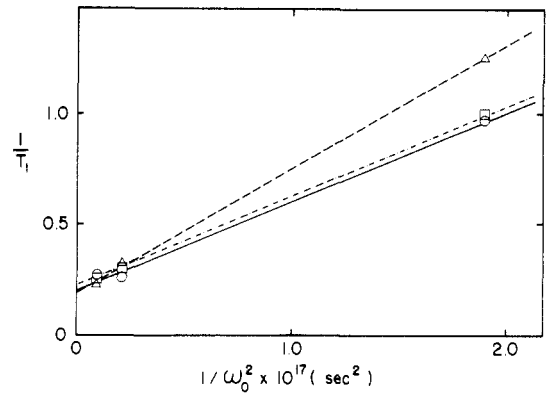

FIGURE 5: Plot of $1/T_1$ vs. $1/\omega_0^2$ for ^{31}P resonances of ATP bound to nitrated G-actin. $1/T_1$ values were determined by using a $(90°-\tau-90°-\tau-90°-\tau$ ...) pulse sequence on nitrated G-actin at 4 °C (same sample as was used in Figure 2). (△) γ-Phosphate; (□) α-phosphate; (○) β-phosphate.

Table III: Analysis of CSA and DD Contributions to T_1 and T_2 for ^{31}P Resonances of ATP Bound to Nitrated G-Actin

frequency (MHz)	$1/T_{2,OBS}$ (s^{-1})	$1/T_{2,DD}$ (s^{-1})	$1/T_{2,CSA}$ (s^{-1})	$1/T_{1,OBS}$ (s^{-1})	$1/T_{1,DD}$ (s^{-1})	$1/T_{1,CSA}$ (s^{-1})	τ_c[a] (ns)	$(\Delta\sigma)(1 + \eta^2/3)^{1/2}$[b] × 10^{-6}
				$P_{\gamma,\beta}$				
36.4	51	29	22	1.27	1.08	0.19	57	280
109.3	120	29	91	0.32	0.13	0.19	40	240
162.0	260	29	231	0.23	0.04	0.19	42	250
				$P_{\alpha,\beta}$				
36.4	51	36	15	1.00	0.77	0.23	43	270
109.3	140	36	104	0.30	0.07	0.23	39	260
162.0	290	36	254	0.27	0.04	0.23	40	260
				$P_{\beta,B}$				
36.4	39	27	12	0.97	0.77	0.20	41	250
109.3	160	27	133	0.26	0.06	0.20	45	260
162.0	290	27	263	0.27	0.07	0.20	44	260

[a] Based on $\tau_c = [^3/_2(T_{1,CSA}/T_{2,CSA})(1/\omega_0^2)]^{1/2}$. [b] Based on $(\Delta\sigma)(1 + \eta^2/3)^{1/2} = [(84.375/\omega_0^2)(1/T_{2,CSA})(1/T_{1,CSA})]^{1/4}$.

Table IV: Principal Values[a] of the ^{31}P Chemical Shielding Tensors of Various Model Compounds

compounds	σ_{11}	σ_{22}	σ_{33}	$^1/_3$ trace[b]	$\Delta\sigma$[c,f]	η[d,f]	$(\Delta\sigma)(1+\eta^2/3)^{1/2}$[e,f]	reference
				Nonesterified Phosphate				
KH_2PO_4	16.5	1.1	1.1	6.2	15.3	0	15.3	Terao & Hashi (1974)
urea–phosphoric acid	27	3	−45	−5	60	0.6	62	Herzfeld et al. (1978)
				Monoester				
5′-AMP $(Na)_2$	78	−29	−29	+7	107	0	107	Terao et al. (1977)
5′-GMP $(Na)_2$	63	−25	−25	+4	88	0	88	Terao et al. (1977)
pyrophosphate $(Na)_4$					127	0	127	Shriver & Sykes (1981)
pyrophosphate $(Ca)_2P(2)$	48	−44	−67	−21	104	0.33	105	Kohler et al. (1976)
5′-AMP (free acid)	77	8	−83	+1	126	0.82	139	Terao et al. (1977)
3′-CMP (free acid)	67	11	−72	+2	111	0.76	121	Terao et al. (1977)
phosphorylethanolamine	67	13	−69	+4	109	0.74	119	Kohler & Klein (1976)
distearoylphosphatidic acid	40	4	−48	−1	70	0.77	77	Kohler & Klein (1977)
				Diester				
poly(A) (K)	89	24	−110	−1	166	0.58	174	Terao et al. (1977)
poly(G) (K)	83	24	−112	−2	166	0.53	173	Terao et al. (1977)
dipalmitoylphosphatidylcholine	81	25	−110	−1	163	0.52	170	Herzfeld et al. (1978)
dipalmitoylphosphatidylethanolamine (anhydrous)	83	21	−103	0	155	0.60	164	Herzfeld et al. (1978)
				Triester				
P_4O_{10}					265	0	265	Luchen & Williams (1969)

[a] All values are in parts per million relative to H_3PO_4, taking upfield as positive. [b] $^1/_3$ trace (ppm) = $^1/_3(\sigma_{11}+\sigma_{22}+\sigma_{33})$. [c] $\Delta\sigma$ (ppm) = $\delta_z - {}^1/_2(\delta_x+\delta_y)$ where δ_x, δ_y, and δ_z are traceless tensor elements (Hull & Sykes, 1975) and δ_z is taken by convention to be the maximum absolute value of δ_{ii} (i = 1, 2, or 3). [d] $\eta = (\delta_x-\delta_y)/\delta_z$. [e] $(\Delta\sigma)(1+\eta^2/3)^{1/2} = |\sigma_{11}-\sigma_\perp|$ if axial symmetry applies.

of the binding of the phosphates of ATP (Cooke & Murdoch, 1973).

In Table III, calculated values of the anisotropy of the chemical shift $(\Delta\sigma)(1+\eta^2/_3)^{1/2}$ are given. When the more accurate values determined at 109.3 and 162 MHz are determined, shielding anisotropies of 240, 260, and 260 ppm for the γ-, α-, and β-phosphates, respectively, were determined. Principal values of the chemical shift tensor for ATP or ADP have not as yet been determined. Values are available for pyrophosphate, a possible model compound for the phosphate of ATP. Early studies using sodium and potassium pyrophosphates yielded a value for $(\Delta\sigma)(1+\eta^2/3)^{1/2}$ of 200 ± 100 ppm, assuming axial symmetry (Derbyshire et al., 1969). More recent studies of the powder pattern of sodium pyrophosphate gave a $(\Delta\sigma)(1+\eta^2/3)^{1/2}$ of 127 ppm (Shriver & Sykes, 1981), and crystal studies of α-$Ca_2P_2O_7$ yielded $(\Delta\sigma)(1+\eta^2/3)^{1/2}$ values of 95 and 105 ppm for the two phosphates (Kohler et al., 1976). Obviously, the shielding anisotropy found for the γ-phosphate of ATP bound to nitrated G-actin is considerably higher than that expected on the basis of either sodium or calcium pyrophosphate.

One approach to the analysis of shielding anisotropies of various organophosphate model compounds is to look at the degree of esterification or protonation of the phosphate (Terao et al., 1977). The principal values of the chemical shift tensors of various model compounds are given in Table 4. The values of $\Delta\sigma$, η, and $(\Delta\sigma)(1+\eta^2/3)^{1/2}$ have been calculated. One can see that the $(\Delta\sigma)(1+\eta^2/3)^{1/2}$ term is about 15–60 ppm for nonesterified phosphates, 80–140 ppm for monoesters, 160–175 ppm for diesters, and 265 ppm for a triester. Protonation has a similar effect to esterification, although not as great in magnitude (Terao et al., 1977). For example, the disodium forms of mononucleotides 5′-AMP and 5′-GMP have $\Delta\sigma$ values of 90–100 ppm, while the addition of a proton leads to the loss of axial symmetry and an increase of the $(\Delta\sigma)(1+\eta^2/3)^{1/2}$ values to 120–140 ppm. This effect has been attributed to the degree of dπ–pπ double bond formation between the phosphorus and the oxygens (Kohler et al., 1976). When an oxygen is involved in an ester linkage, it has less electron density in its pπ orbitals to contribute toward this double bond while the remaining nonbridging oxygens have a concomitant increase in dπ–pπ double bond formation. Thus, esterification results in an anisotropy of double bond character among the P–O bonds and hence an uneven distribution of electron density around the phosphorus. The chemical shift anisotropy terms for the ATP bound to nitrated G-actin $[(\Delta\sigma)(1+\eta^2/3)^{1/2}$ of 240 to 260 ppm] are higher than would be expected for phosphate monoesters or diesters and are almost as high as measured for the model phosphate triester P_4O_{10}. This may indicate that the electronic structure of the bound ATP has triester-like characteristics. Related to the nature of the P–O bond hybridization is the O–P–O bond angle. While PO_4^{3-} is a regular tetrahedron with all bond angles equal to 109.5°, the O–P–O bond angles are 101.5° between the bridging and nonbridging oxygens of P_4O_{10} and 116.5° between the two bridging oxygens. The O–P–O bond angles have been shown to have dramatic effects on the overall chemical shifts of phosphate compounds (Gorenstein, 1975; Gorenstein & Kar, 1975). It is quite likely that the binding of ATP to nitrated G-actin results in some changes in the O–P–O bond angles, due to interactions of the ATP with the protein. These bond angle changes could dramatically affect individual elements of the chemical shift tensor, leading to a large chemical shift anisotropy, while the overall averaged chemical shift value is only altered by a few parts per million relative to free ATP.

While numerous ^{31}P NMR studies of ATP bound to various proteins have been done (Cohn & Nageswara Rao, 1980; O'Neil & Richards, 1980), field-dependent studies have usually not been done. One exception is the study of the binding of ATP to yeast 3-phosphoglycerate kinase (Nageswara Rao & Cohn, 1978). The line widths of the resonances for ATP bound to this protein are reported to be about 8 Hz at 40.3 MHz and 40–45 Hz at 109.3 MHz. Plotting $1/T_2$ vs. ω_0^2, we found that about 95% of the line width at 109.3 MHz is due to CSA. Yeast 3-phosphoglycerate kinase has a mo-

lecular weight of 45 000–46 000 (Scopes, 1973), which is close to the molecular weight of G-actin (M_r 42 300). If we assume that 3-phosphoglycerate kinase has approximately the same diameter as G-actin, we can calculate a τ_c of 39 ns at 1 °C on the basis of the Stokes–Einstein equation. From the value of $1/T_{2,CSA}$ and this τ_c for 3-phosphoglycerate kinase, we can estimate a value for $(\Delta\sigma)(1 + \eta^2/3)^{1/2}$ of 265–285 ppm for ATP bound to this enzyme. This screening anisotropy is slightly greater than our values for ATP bound to nitrated G-actin. Thus, there may well be a general trend toward much higher chemical shift anisotropies for protein-bound ATP than anticipated on the basis of studies of model compounds free in solution.

One possible contribution to the observed line width (and hence $1/T_{2,OBS}$) and to the observed spin–lattice relaxation rate ($1/T_{1,OBS}$) is chemical exchange. Since both the free and protein-bound ATP resonance can be clearly seen (Figure 1), the exchange of ATP between these two sites must be slow with respect to T_2 processes [see Brauer & Sykes (1981)]. Figure 3 shows the 36.4-MHz NMR spectrum of ATP bound to nitrated G-actin at 4 and at 28 °C; the fact that the bound resonances do not exhibit an increase in line width (±3 Hz) indicates that the system is in the slow exchange limit at 4 °C. The contribution of chemical exchange to the line width of the bound ATP resonance is k_{-1}/π. Since an increase in the temperature did not result in a measurable increase in line width, k_{-1} must be much smaller than $1/T_{2B}$ (14–50 s^{-1} at 36.4 MHz). Typical literature values for the k_{-1} of ATP on G-actin range from 6×10^{-5} s^{-1} to 1.2×10^{-4} s^{-1} (Strzelecka-Golaszewska, 1973; Neidl & Engel, 1979; Hitchcock, 1980). Since these published k_{-1} values are indeed much less than the line widths of the bound ATP resonances, our results are in good accord with the literature.

The exchange of ATP between its free and bound sites is also slow relative to T_1 relaxation processes since quite different T_1 values for the resonances of free and protein-bound ATP were obtained (see Table II). If fast exchange with respect to T_1 were true, both free and protein-bound ATPs would have the same observed T_1 value, a weighted average value of the free T_1 and bound T_1. The corresponding contribution of chemical exchange to the $1/T_1$ of a protein-bound ATP resonance in the slow exchange case is k_{-1}. Even at higher magnetic field strengths where $1/T_{1,OBS}$ is low (0.23–0.27 s^{-1} at 162.0 MHz), the literature values for k_{-1} of 10^{-5}–10^{-4} s^{-1} are too small to appreciably effect the measured $1/T_1$. Thus, the exchange of ATP between its free and bound sites is in the slow exchange limit with respect to both T_1 and T_2 and hence does not contribute significantly to either $1/T_{2,OBS}$ or $1/T_{1,OBS}$.

We can obtain some information about the nitrated G-actin–ATP complex from the homonuclear spin–spin splitting patterns. From the 36.4-MHz NMR spectra of nitrated G-actin, the $^2J_{P_\alpha, P_\beta}$ splitting was found to be 12 ± 2 Hz and the $^2J_{P_\beta, P_\gamma}$ splitting was found to be 20 ± 2 Hz (see Figure 3). Free ATP (not complexed to any protein or metal ion) has a splitting of $^2J_{P_\alpha, P_\beta} = {}^2J_{P_\beta, P_\gamma} = 19.6$ Hz under the same conditions of temperature and pH, while the Ca–ATP complex has a splitting of $^2J_{P_\alpha, P_\beta} = {}^2J_{P_\beta, P_\gamma} = 17.0$ Hz (Brauer & Sykes, 1981). Thus, the binding of ATP to nitrated G-actin has resulted in a dramatic alteration of the $^2J_{P_\alpha, P_\beta}$ coupling constant but not of the $^2J_{P_\beta, P_\gamma}$ coupling constant. A similar decrease in both geminal coupling constants of about 5 Hz was found for the binding of ATP to adenylate kinase plus Mg^{2+} (Nageswara Rao et al., 1978). Geminal coupling constants for YO_2P–O–PO_2Y model compounds are believed to be negative and tend to decrease in magnitude as the electronegativity of the substituent Y increases (Finer & Harris, 1970). (Back-donation of electron density from the substituents is, however, a complicating process.) The decrease in the $^2J_{P_\alpha, P_\beta}$ coupling constant of ATP upon binding to nitrated G-actin can be explained in terms of an electrophilic group interacting with the nonbridging oxygens of the phosphates of ATP, increasing the electronegativity of these oxygens.

The role of CSA as a dominant mechanism in both T_1 and T_2 relaxation rates of ^{31}P nuclei at high magnetic field strengths has been generally underestimated. While this mechanism does limit the increase in resolution of ^{31}P resonances with higher magnetic fields, it can provide important information pertaining to molecular motions and electronic structures of phosphorus-containing metabolites, coenzymes, allosteric effectors, phospholipids, and polynucleotides. Cross-relaxation between ^1H and ^{31}P resonances does not significantly influence the T_1 values of the ^{31}P resonances in the nonextreme narrowing limit.

Acknowledgments

We are greatly indebted to Dr. L. B. Smillie for amino acid analyses and Drs. C. Kay and W. McCubbin for their advice in preparation of the G-actin. We also thank Drs. Tom Nakashima, G. Bigam, and Tom Brisbane for their help in the use of the Bruker WH-400/DS, Bruker WH-200, and Bruker HFX10 NMR spectrometers and Gerard McQuaid for his meticulous upkeep of the 270-MHz spectrometer.

References

Abragam, A. (1961) *Principals of Nuclear Magnetism*, Oxford University Press, London and New York.

Adelstein, R. S., Godfrey, J. E., & Kielly, W. W. (1963) *Biochem. Biophys. Res. Commun. 12*, 34–38.

Brauer, M., & Sykes, B. D. (1981) *Biochemistry 20*, 2060–2064.

Campbell, I. D., & Freeman, R. (1973) *J. Magn. Reson. 11*, 143–162.

Carlsson, L., Nystom, L.-E., Sundkrist, I., & Morkey, F., & Lindberg, U. (1977) *J. Mol. Biol. 115*, 465–483.

Chantler, P. D., & Gratzer, W. B. (1975) *Eur. J. Biochem. 60*, 67–72.

Cheung, H. C., Cooke, R., & Smith, L. (1971) *Arch. Biochem. Biophys. 142*, 333–339.

Clarke, M., & Spudich, J. A. (1977) *Annu. Rev. Biochem. 46*, 797–823.

Cohen, C. M., & Branton, D. (1979) *Nature (London) 279*, 164–165.

Cohn, M., & Nageswara Rao, B. D. (1980) *Bull. Magn. Reson. 1*, 1–60.

Cooke, R., & Murdoch, L. (1973) *Biochemistry 12*, 3927–3932.

Cozzone, P. J., Nelson, D. J., & Jardetzky, O. (1974) *Biochem. Biophys. Res. Commun. 60*, 341–347.

Derbyshire, J. P., Stuart, J. P., & Warner, D. (1964) *Mol. Phys. 17*, 449–455.

Ebashi, S., & Ebashi, F. (1965) *J. Biochem. (Tokyo) 58*, 7–12.

Elzinga, M. (1971) 162nd National Meeting of the American Chemical Society, Washington, D.C., Abstr. 234.

Engel, J., Fasold, H., Hulla, F. W., Waechten, F., & Wagner, A. (1977) *Mol. Cell. Biochem. 18*, 3–13.

Finer, E. G., & Harris, R. K. (1970) *Prog. Nucl. Magn. Reson. Spectrosc. 6*, 61–118.

Freeman, R., & Hill, H. D. W. (1971) *J. Chem. Phys. 54*, 3367–3377.

Gorenstein, D. G. (1975) *J. Am. Chem. Soc. 97*, 898–900.

Gorenstein, D. G., & Kar, D. (1975) *Biochem. Biophys. Res. Commun. 65*, 1073–1080.
Grazi, E., & Magri, E. (1979) *FEBS Lett. 104*, 284–286.
Gutowsky, H., & Woessner, D. E. (1956) *Phys. Rev. 104*, 843–845.
Herzfeld, J., Griffin, R. G., & Haberkorn, R. A. (1978) *Biochemistry 17*, 2711–2722.
Hitchcock, S. E. (1980) *J. Biol. Chem. 255*, 5668–5673.
Hull, W. E., & Sykes, B. D. (1975a) *J. Mol. Biol. 98*, 121–153.
Hull, W. E., & Sykes, B. D. (1975b) *J. Chem. Phys. 63*, 867–880.
Hull, W. E., Halford, S. E., Gulfreund, H., & Sykes, B. D. (1976) *Biochemistry 15*, 1547–1561.
Huxley, H. E. (1967) *Science (Washington, D.C.) 64*, 1356–1366.
Ikkai, F., Wahl, P., & Akushet, J.-C. (1979) *Eur. J. Biochem. 93*, 397–408.
Kohler, S. J., & Klein, M. P. (1976) *Biochemistry 15*, 967–973.
Kohler, S. J., & Klein, M. P. (1977) *Biochemistry 16*, 519–524.
Kohler, S. J., Ellett, J. D., & Klein, M. P. (1976) *J. Chem. Phys. 64*, 4451.
Laki, K., Bowern, W. Y., & Clark, A. (1950) *J. Gen. Physiol. 33*, 437–443.
Lazarides, E., & Lindberg, U. (1974) *Proc. Natl. Acad. Sci. U.S.A. 71*, 4742–4746.
Lehrer, S. S. & Elzinga, M. (1972) *Fed. Proc., Fed. Am. Soc. Exp. Biol. 31*, 502.
Luchen, E. A. L., & Williams, D. F. (1969) *Mol. Phys. 16*, 17–23.
Mannherz, H. G., & Goody, R. S. (1970) *Annu. Rev. Biochem. 45*, 427–465.
McCubbin, W. D., & Kay, C. M. (1980) *Acc. Chem. Res. 13*, 185–192.
Mihashi, K., & Wahl, P. (1975) *FEBS Lett. 52*, 8–12.
Nageswara Rao, B. D., & Cohn, M. (1978) *J. Biol. Chem. 253*, 8056–8060.
Nageswara Rao, B. D., Cohn, M., & Noda, L. (1978) *J. Biol. Chem. 253*, 1149–1158.
Neidl, C., & Engel, J. (1979) *Eur. J. Biochem. 101*, 163–169.
Nelson, D. J., Cozzone, P. J., & Jardetzky, O. (1974) *Jerusalem Symp. Quant. Chem. Biochem. 7*, 501–513.
O'Neill, I. K., & Richards, C. P. (1980) *Annu. Rep. NMR Spectrosc. 10A*, 133–236.
Oosawa, F., & Kasai, M. (1971) *Biol. Macromol. 5*, 261–322.
Pollard, T. D., & Weihing, R. R. (1974) *CRC Crit. Rev. Biochem. 2*, 1–65.
Rees, M. K., & Young, M. (1967) *J. Biol. Chem. 242*, 4449–4458.
Scopes, R. K. (1973) *Enzymes, 3rd Ed. 8*, 335–351.
Shriver, J. W., & Sykes, B. D. (1981) *Biochemistry 20*, 2004–2012.
Solomon, I. (1955) *Phys. Rev. 99*, 559–565.
Spudich, J. A., & Watt, S. (1971) *J. Biol. Chem. 246*, 4866–4871.
Straub, F. B., & Feuer, G. (1950) *Biochim. Biophys. Acta 4*, 455–470.
Strzelecka-Golaszewska, H. (1973) *Eur. J. Biochem. 37*, 434–440.
Sykes, B. D., Hull, W. E., & Snyder, G. H. (1978) *Biophys. J.*, 137–146.
Tao, T. (1978) *FEBS Lett. 93*, 146–150.
Terao, T., & Hashi, T. (1974) *J. Phys. Soc. Jpn. 36*, 989–996.
Terao, T., Matsui, S., & Ahasura, K. (1977) *J. Am. Chem. Soc. 99*, 6136–6138.
Vincent, J. P., Luzdunski, M., & Delage, H. (1970) *Eur. J. Biochem. 12*, 250–260.
Weber, K., & Osborn, M. (1969) *J. Biol. Chem. 244*, 4406–4412.
Werbelow, L. B., & Marshall, A. G. (1974) *Mol. Phys. 28*, 113–127.
Werbelow, L. B., & Marshall, A. G. (1975) *J. Magn. Reson. 11*, 143–154.
Withers, S. G., Sykes, B. D., Madsen, N. B., & Kasvinsky, P. J. (1979) *Biochemistry 18*, 5342–5348.